Second International Workshop on ERS SAR Interferometry, FRINGE '99, 10–12 Nov 1999, Liège, Belgium

Development of a stochastic model for repeat-pass SAR interferometry

Ramon Hanssen and Roland Klees
Delft Institute for Earth-Oriented Space Research, Delft University of Technology,
P.O. Box 5030, 2600 GA Delft, The Netherlands
hanssen@geo.tudelft.nl

ABSTRACT

A mathematical model for the estimation of topographic height or surface deformation is presented, consisting of a functional and a stochastic model. Atmospheric signal is modeled as an isotropic covariance function and included in the stochastic model. This procedure yields a standardized definition for parameter estimation from repeat-pass radar interferometry.

INTRODUCTION

Repeat-pass radar interferometry can be used for the recovery of topography or surface deformation on earth from random interferometric phase observations φ_k, with $k = i + (i-1)j$, where i and j represent the row and column of the interferogram, respectively. For every observation, at least five unknown parameters need to be estimated:

- topographic height H_k,
- deformation in slant direction D_k
- slant atmospheric delay during acquisition 1: $S_k^{t_1}$,
- slant atmospheric delay during acquisition 2: $S_k^{t_2}$, and
- integer ambiguity number w_k.

Therefore, the problem is ill-posed and underdetermined. The observed phase values φ_k form a real stochastic vector of observations $\boldsymbol{\varphi} \in \mathbb{R}^n$, characterized by the first moment $E\{\boldsymbol{\varphi}\}$ and the second moment $D\{\boldsymbol{\varphi}\}$. Then, after linearization, the relation between the observations and the unknown parameters can be written as a Gauss-Markoff model (Koch 1999):

$$E\{\boldsymbol{\varphi}\} = \mathbf{A}\mathbf{x}; \quad D\{\boldsymbol{\varphi}\} = \mathbf{C}_{\boldsymbol{\varphi}} = \sigma^2 \mathbf{Q}_{\boldsymbol{\varphi}}, \tag{1}$$

where $\mathbf{A}$ is the design matrix, $\mathbf{C}_{\boldsymbol{\varphi}}$ is the variance-covariance matrix, $\mathbf{Q}_{\boldsymbol{\varphi}} \in \mathbb{R}^{n \times n}$ the real positive-semidefinite $n \times n$ cofactor matrix, and $\sigma^2 \in \mathbb{R}^+$ the a priori variance factor. The vector of parameters $\mathbf{x} \in \mathbb{R}^{5n}$ is assumed to be real and non-stochastic.

Tailoring the model for repeat-pass interferometry we can write the system of linearized observation equations, or *functional model* as

$$E\{\begin{bmatrix} \varphi_1 \\ \varphi_2 \\ \vdots \\ \varphi_n \end{bmatrix}\} = \begin{bmatrix} \mathbf{A}_1 & & & \\ & \mathbf{A}_2 & & \\ & & \ddots & \\ & & & \mathbf{A}_n \end{bmatrix} \begin{bmatrix} \mathbf{x}_1 \\ \mathbf{x}_2 \\ \mathbf{x}_3 \\ \vdots \\ \mathbf{x}_n \end{bmatrix} \tag{2}$$

where $\mathbf{A}_k$ is the part of the design matrix corresponding to observation k, defined as:

$$\mathbf{A}_k = \begin{bmatrix} \frac{4\pi}{\lambda}\frac{R_k \sin\theta_k}{B_k^{\perp}}, & \frac{4\pi}{\lambda}, & \frac{4\pi}{\lambda}, & -\frac{4\pi}{\lambda}, & -2\pi \end{bmatrix}, \tag{3}$$

and the parameter vector $\mathbf{x}_k$ corresponding to observation k is:

$$\mathbf{x}_k = \begin{bmatrix} H_k, & D_k, & S_k^{t_1}, & S_k^{t_2}, & w_k \end{bmatrix}^T. \tag{4}$$

The dispersion of the vector of observations can be estimated using empirical coherence measurements or system theoretical considerations, and the diagonal variance-covariance matrix $\mathbf{C}_{\boldsymbol{\varphi}}$ can be written as:

$$\mathbf{C}_{\boldsymbol{\varphi}} = \begin{bmatrix} \sigma_1^2 & & & \\ & \sigma_2^2 & & \\ & & \ddots & \\ & & & \sigma_n^2 \end{bmatrix} = \sigma^2 \mathbf{Q}_{\boldsymbol{\varphi}}, \quad (\sigma^2 = 1), \tag{5}$$

where σ_k^2 can be approximated using the estimated coherence values from the coregistered SAR data. We assume that there is no correlation between the phase observations in the interferogram.

In this form, design matrix $\mathbf{A}$ has a rank defect of $4n$. To solve this problem either (i) deterministic information needs to be introduced, or (ii) the model has to be rephrased.

Regarding possibility (i), we assume that either topography H_k, or deformation D_k are known. Moreover, for now we assume that the integer ambiguity number w_k is known as well, i.e., phase unwrapping can be performed perfectly. Nonetheless, both assumptions can only reduce the rank deficiency from $4n$ to $2n$, which makes the system still not solvable. Therefore, we propose to apply possibility (ii), and rephrase the

model by lumping the atmospheric slant delay signal into one parameter $S_k = S_k^{t1} - S_k^{t2}$, transferring this parameter to the stochastic model and replace $\mathbf{C}_{\varphi}$ by

$$\mathbf{C} \doteq \mathbf{C}_{\varphi} + \mathbf{C}_{\mathbf{s}}, \tag{6}$$

where $\mathbf{C}_{\mathbf{s}}$ is the variance-covariance matrix of the atmospheric delay parameter S_k. Using this approach, the design matrix $\mathbf{A}$ has full rank. Proper definition of $\mathbf{C}$ in terms of measurement noise and atmospheric noise provides the necessary tools for data adjustment and filtering. In the following sections, the characteristics of the atmospheric error signal are discussed.

ATMOSPHERIC ERROR SIGNAL

The influence of the refractivity distribution in the atmosphere is apparent in two distinct phenomena: vertical stratification and turbulent mixing.

- Vertical stratification is the result of different vertical (1D) refractivity profiles during both SAR acquisitions, assuming that there are no heterogeneities within one horizontal layer. This affects mountainous terrain only.
- Turbulent mixing results from convective processes in the boundary layer and causes spatial (3D) heterogeneity in the refractivity during both acquisitions. This affects flat terrain as well as mountainous terrain.

Empirical studies of the effect of vertical stratification in the presence of topography have been discussed by Hanssen and Klees (1999). The error propagation induced by vertical stratification can only be performed when initial topographic heights are known or derived in an iterative way. If such information is available, the covariance between two points in the image at a different height level could be inserted in $\mathbf{C}_{\mathbf{s}}$. Here we will focus on the consequences of turbulent mixing.

The effect of turbulent mixing, resulting in 3D spatial heterogeneity of refractivity, is a general form of atmospheric disturbance, affecting all types of space-geodetic radio observations (e.g. VLBI, GPS, INSAR). On short spatial scales the dominant signal is caused by water vapor variability. Fig. 1 shows the turbulent signal in eight differential tandem interferograms, acquired over the Netherlands during 1995/96. The interferometric phase is unwrapped and converted to zenith delay signal in mm.

The windows in the data of Fig. 1 are used to calculate a set of power spectra. First the mean value of the window is subtracted, and both in azimuth and in range direction a linear trend is removed from the data. A 2D FFT is performed and squared to obtain the power spectrum. Assuming isotropic behavior, all wavenumbers u, v are binned into radial wavenumbers q, using $q^2 = u^2 + v^2$, and summed, yielding the radially averaged 1D power spectrum. For all eight interferograms of Fig. 1, the resulting spectra are shown in Fig. 2. The diagonal lines in Fig. 2 indicate the slope

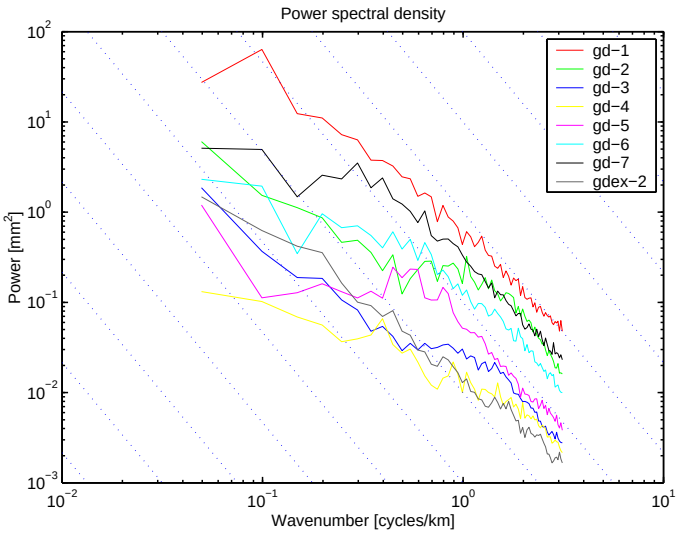

Figure 2: The 1D rotationally averaged power spectra of the eight atmospheric situations in Fig. 1. The diagonal lines indicate $-8/3$ power law behavior.

of $-8/3$ power law functions. The data show that all atmospheric situations exhibit power law behavior, although the slopes may differ between $-5/3$ and $-8/3$ for different scale regimes. Furthermore, there is a one order of magnitude range in the vertical position of the spectra, indicating more or less severe atmospheric situations. The red line is corresponding with the first interferogram in Fig. 1, which indeed exhibits the most severe zenith delay variability.

In analyzing these atmospheric signals, we assume second-order stationarity, which implies that the covariance between two observations is a function only of the distance between the observations. Empirical covariance functions $C(r)$, where r reflects the distance between two observations, are now derived from the inverse FFT of the power spectra, as shown in Fig. 3. Clearly, the interferogram with the most severe atmospheric signal shows the most dominant empirical covariance function.

The standard approach to modeling the covariance function is by approximating some parametric analytical form for $C(r)$ which ensures positive-definiteness (Rummel 1990; Daniels and Cressie 1999). As a first, rather coarse attempt we use a Gaussian (Moritz 1989)

$$C(r) = C_0 e^{-A^2 r^2}, \tag{7}$$

with $A^2\eta^2 = \ln 2$, where η is the correlation length. The analytical covariance functions corresponding to

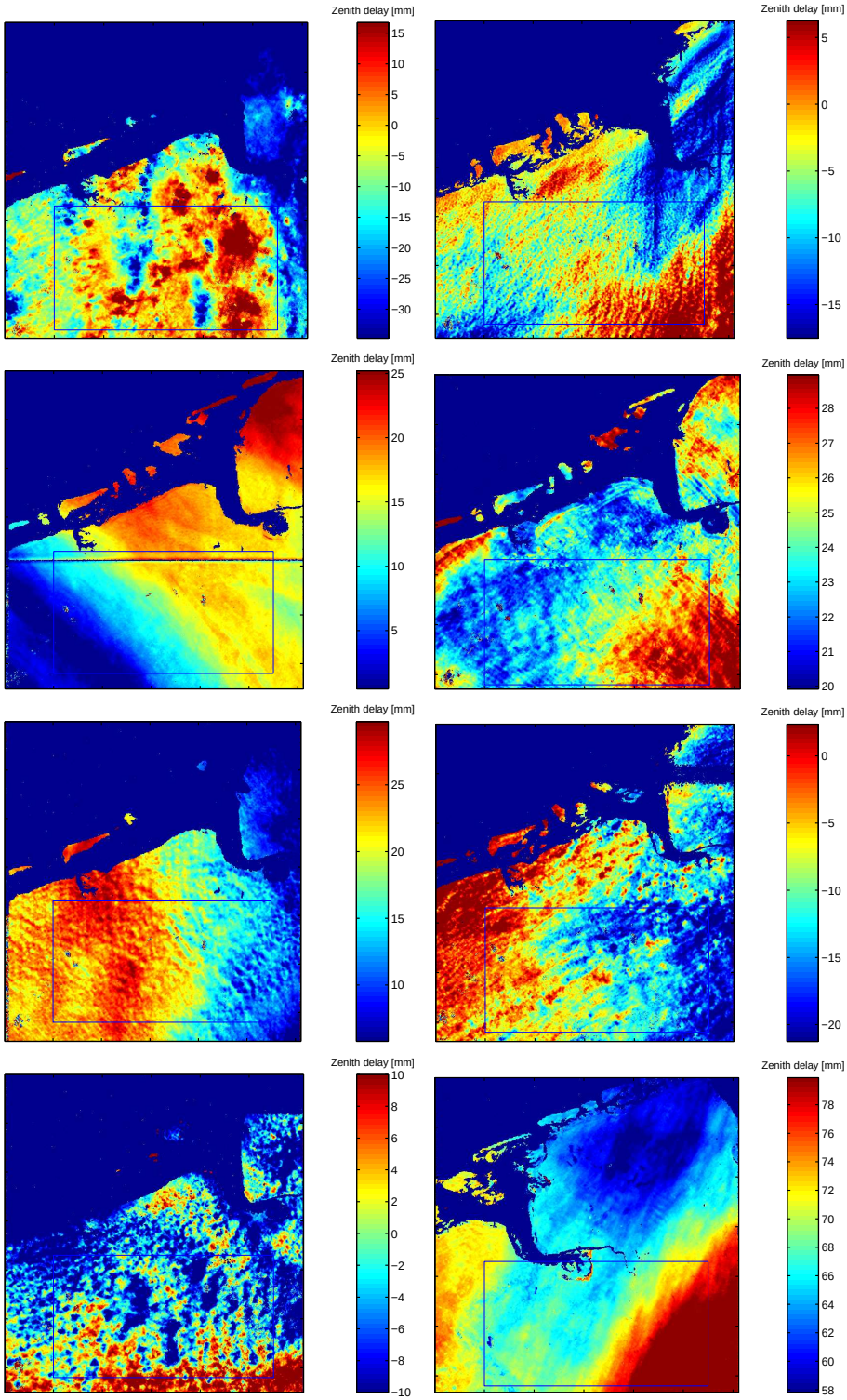

Figure 1: Eight arbitrary differential tandem interferograms showing only atmospheric signal. The interferograms are acquired in [month/year] 7/95, 8/95, 12/95, 3/96, 4/96, 5/96, 8/96, 2/96

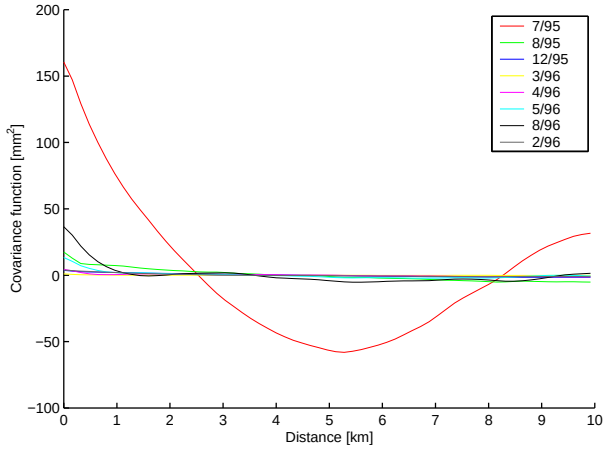

Figure 3: Empirical covariance functions corresponding to the atmospheric situations of Fig. 1, derived from the power spectra.

the empirical functions in Fig. 3 are shown in Fig. 4. Without any a priori knowledge of the state of the

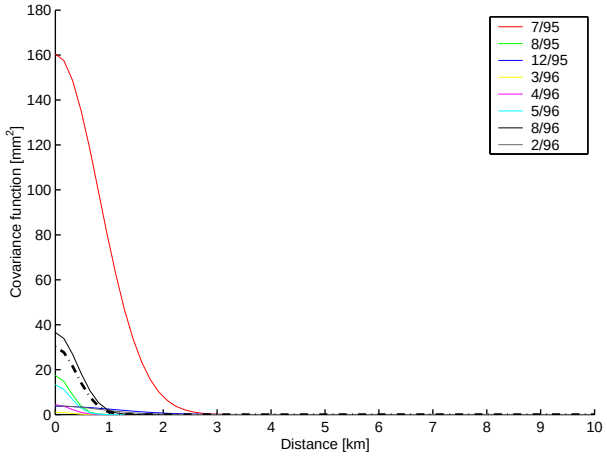

Figure 4: Analytical positive-definite covariance functions derived from the empirical covariance function shown in Fig. 3. The dotted line indicates a mean covariance function based on all eight realizations.

atmosphere during two SAR acquisitions a mean covariance function, as depicted by the striped-dotted line in Fig. 4, seems an appropriate first-order choice to model the variance of the atmospheric signal. Note, however, that some knowledge on atmospheric convectivity might result in a more sophisticated choice for the covariance parameters. Such information might be obtained from, e.g., cloud type observations.

The final step in constructing the variance-covariance matrix $\mathbf{C_s}$ of the atmospheric delay, cf. eq. 6, is to determine the horizontal distance between every pair of observations, and fill in the covariance corresponding to that distance at the appropriate position in $\mathbf{C_s}$. The result of this procedure is shown in Fig. 5. The

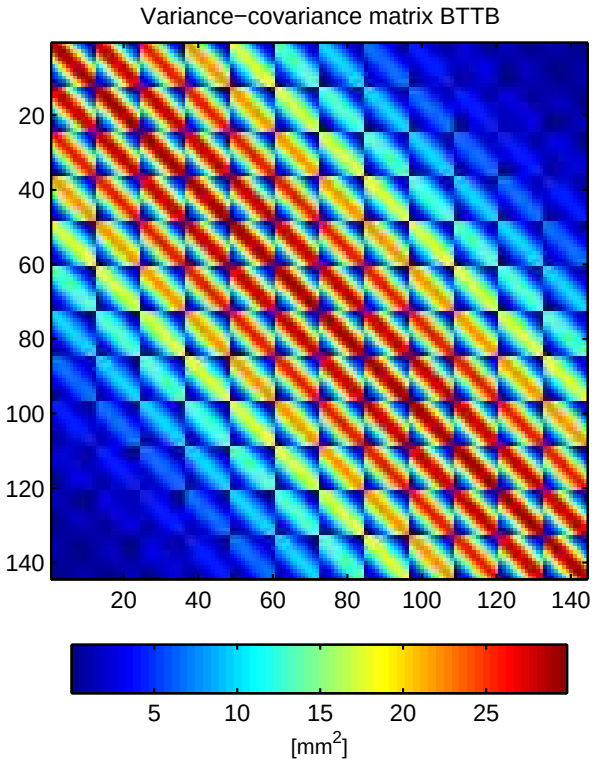

Figure 5: Variance-covariance matrix $\mathbf{C_s}$, obtained for the vectorized observations $\boldsymbol{\varphi}$, using the mean covariance function of Fig. 3. A 12×12 interferogram is assumed, with a pixel size of 0.16 km. The matrix exhibits a Block Toeplitz-Toeplitz Block (BTTB) structure.

first column of this matrix corresponds with all combinations of observations with observation φ_1, at the upper left position in the original interferogram. Since the vectorization of the observations is performed as described in the introduction, the covariance behavior for observations in the same column of the interferogram is smooth, whereas the step to the next column of the interferogram is a discrete transition. Performing this procedure for all combinations with all observations, we find $\mathbf{C_s}$ as in Fig. 5. Note that for this example, a very small interferogram of 12×12 pixels was simulated, with a pixel size of approximately 200 m. It is obvious how the number of elements in the $\mathbf{C_s}$-matrix increases quadratically with an increase of the interferogram size.

The structure of $\mathbf{C_s}$ is a Block Toeplitz matrix with Toeplitz blocks (BTTB). In Fig. 5, matrix $\mathbf{C_s}$ is a 12×12 block matrix, each block being a 12×12 Toeplitz matrix (Strohmer 1997). For BTTB matrices, fast inversion techniques exist, see, e.g.,Kailath, Vieira, and Morf (1978),Bitmead and Anderson (1980),Strang

(1986), Ammar and Gragg (1988), and Strohmer (1997).

CONCLUSIONS

The problem of solving parameters such as topographic height or deformation signal from radar interferograms is described in a mathematical form, identifying a functional and a stochastic model. Rank defects in the system of equations are solved by defining an analytical covariance function for the atmospheric signal, based on a set of differential interferograms. This procedure yields a combined variance-covariance matrix, consisting of a diagonal variance matrix based on coherence observations only, and a block Toeplitz-Toeplitz block covariance matrix based on atmospheric signal. Future work will focus on the verification and validation of these models, and solving the numerical restrictions for these very large matrices. Ideally, this parameterization should allow series of interferograms to be combined in the same model, to allow solving for the unknown parameters in one inversion procedure.

References

Ammar, G. S. and W. B. Gragg (1988, January). Superfast solution of real positive definite Toeplitz systems. *SIAM J. Matrix Anal. Appl, 9*(1), 61–76.

Bitmead, R. R. and B. D. O. Anderson (1980). Asymptotically fast solution of Toeplitz and related systems of linear equations. *Linear Algebra and Its Applications 34*, 103–116.

Daniels, M. J. and N. Cressie (1999). A hierarchical approach to covariance function estimation for time series. submitted.

Hanssen, R. and R. Klees (1999). An empirical model for the assessment of DEM accuracy degradation due to vertical atmospheric stratification. In *Second International Workshop on ERS SAR Interferometry, FRINGE'99, 10–12 Nov 1999, Liège, Belgium*, pp. 5. ESA.

Kailath, T., A. Vieira, and M. Morf (1978, January). Inverses of Toeplitz operators, innovations, and orthogonal polynomials. *SIAM Review 20*(1), 106–119.

Koch, K.-R. (1999). *Parameter Estimation and Hypothesis Testing in Linear Models* (2 ed.). New York: Springer-Verlag.

Moritz, H. (1989). *Advanced Physical Geodesy* (2 ed.). Karlsruhe: Wichmann verlag.

Rummel, R. (1990). *Physical Geodesy 2, Lecture Notes*. Delft: Delft University of Technology, Department of Geodetic Engineering.

Strang, G. (1986). A proposal for Toeplitz matrix calculations. *Studies in applied mathematics 74*, 171–176.

Strohmer, T. (1997, April). Comutationall attractive reconstruction of bandlimited images from irregular samples. *IEEE Trans. on Geoscience and Remote Sensing 6*(4), 540–548.